The Abdus Salam
International Centre for Theoretical Physics

United Nations
Educational, Scientific and
Cultural Organization

IAEA
International Atomic Energy Agency

2152-15

Joint ICTP-IAEA Course on Natural Circulation Phenomena and Passive Safety Systems in Advanced Water Cooled Reactors

17 - 21 May 2010

COMPUTATIONAL FLUID DYNAMICS FOR NATURAL CIRCULATION: NEEDS & VERIFICATION AND VALIDATION

Yassin A. Hassan
Texas A&M University
College Station
USA

IAEA Course on Natural Circulation in Water-Cooled Nuclear Power Plants,
International Centre for Theoretical Physics (ICTP), Trieste, Italy
17th to 21th May 2010, Paper ID. T27 and T28

COMPUTATIONAL FLUID DYNAMICS FOR NATURAL CIRCULATION: NEEDS & VERIFICATION ANDVALIDATION

Yassin A. Hassan

Texas A&M University, College Station, USA, Email: y-hassan@tamu.edu

KEY WORDS

CFD, turbulence, Reynolds stress, large eddy simulation, mixing, natural circulation

LECTURE OBJECTIVES

The main objective of this lecture is to present a need and the importance of Computational Fluid Dynamics (CFD) simulation for the complex natural circulation phenomena in water cooled nuclear plant components. Examples of CFD simulations of natural circulations are given. However, confidence in the CFD calculations should be assessed. Verification and validation (V&V) are the major processes for assessing and quantifying this confidence. A brief review of V&V terminology and approaches will be discussed.

1. INTRODUCTION

The Computational Fluid Dynamics (CFD) is one of the branches of fluid mechanics that uses numerical methods and algorithms to solve and analyze problems that involve fluid flows. The CFD is a part of computational mechanics which is a part of simulation techniques. The implementation of early-stage simulation tools, specifically CFD, is an international and interdisciplinary trend that allows engineers/designers to computer-test concepts all the way through the development of a process or system. CFD are extending into various industries for modeling industrial processes, performing comprehensive analyses and optimizing the efficiency and cost effectiveness of the new systems and processes. Computers are used to perform the millions of calculations required to simulate and describe fluid dynamic phenomena and the fluid interaction with the complex surfaces used in engineering. The simulations are performed under assumed or measured boundary conditions (geometry, initial states, loads, etc.). Most flows encountered in practical engineering-type applications are geometrically and fluid dynamically complex (three-dimensional, turbulent, unsteady). The fundamental basis of any CFD problem is the Navier-Stokes equations, which define any single-phase fluid flows. These equations can be simplified by removing terms such as those describing viscosity to yield Euler equations. However, even with simplified equations and high speed supercomputers, only approximate solutions can be achieved in many cases. Accurate CFD computer programs that can simulate complex scenarios such as turbulent flows are an ongoing challenging area of research.

Reactor Safety Analysis related to both Pressurized Water Reactors (western type and VVER type) and Boiling Water Reactors mainly relied in a first step on system codes where the primary (and secondary) flows are modeled with a rather coarse nodalization including about hundred mesh points or “control volumes”. Several large system codes such as RELAP [1], CATHARE [2], and TRAC [3] among others have been developed and continuously improved during time have been the major,

universally used tools. These codes are usually based on the two-fluid (six) equation model and are based on interpenetrating-media approach. Most of the analysis using system codes is one-dimensional. However, a much finer resolution of the simulation tools is required. These issues are related to situations where three-dimensional aspects of the flow and geometrical effects have a significance influence on the safety criteria. Turbulent mixing is a feature of these flows and the degree of mixing controls the results such as natural circulation which directly impact the safety. Another example is the counter-current and circulation flow in the downcomer of pressurized water reactors (PWRs) where 1-D assumption during the refill and natural circulation phases results into wrong scenario predictions in the absence of three-dimensional (3D) simulation.

This article will begin with a brief discussion of single-phase flow conservation equations; then, multiphase flow governing equations will be addressed.

2. CONSERVATION EQUATIONS

2.1 Single-Phase Conservation Equations

The Navier-Stokes equations (NSE) for a single-phase flow in space-time (x, t) domain that describe the motion of fluid substances such as liquids and gases can be expressed in differential equations as [4]:

Continuity: $$\frac{\partial \rho}{\partial t} + \nabla \cdot (\rho \mathbf{u}) = 0 \quad (1)$$

Momentum conservation:

$$\rho \frac{\partial \mathbf{u}}{\partial t} + \rho \mathbf{u} \cdot \nabla \mathbf{u} = -\nabla p + \nabla \cdot \boldsymbol{\tau} + \rho \mathbf{f} \quad (2)$$

Energy conservation:

$$\rho \frac{\partial}{\partial t}\left(e + \tfrac{1}{2}u^2\right) + \rho \mathbf{u} \cdot \nabla \left(e + \tfrac{1}{2}u^2\right) = -\nabla \cdot (p\,\mathbf{u}) + \nabla \cdot (\boldsymbol{\tau} \cdot \mathbf{u}) - \nabla \cdot \mathbf{q} + \rho\, \mathbf{f} \cdot \mathbf{u} + \dot{q} \quad (3)$$

where ρ, $\mathbf{u}$, p, and e, which are solutions to these governing equations with the equation of state, are density, velocity, thermodynamic pressure, and specific internal energy, respectively and $\mathbf{f}$ and $\dot{q}$ are body force per mass and internal heating per volume. For the Newtonian fluid shear-stress tensor $\boldsymbol{\tau}$ is given as

$$\boldsymbol{\tau} = \lambda (\nabla \cdot \mathbf{u}) \boldsymbol{\delta} + \mu \left(\nabla \mathbf{u} + \nabla \mathbf{u}^T\right)$$

where $\boldsymbol{\delta}$ is a unit tensor and μ and λ are (first coefficient of) viscosity and second coefficient of viscosity, respectively. $\nabla \mathrm{u}^T$ is the "transpose" of the velocity gradient tensor. Also, according to the Fourier's law heat flux $\mathbf{q}$ is given as

$$\mathbf{q} = -\kappa \nabla T$$

where T and κ are temperature and thermal conductivity, respectively.

2.2 Turbulence Modeling

Nature is characterized by three dimensional flows and turbulence plays a predominant part in the in the development of these flows. Turbulence flows have properties that make it difficult to develop an accurate tractable theory. The velocity field U(x, t) is three-dimensional, time-dependent and random. The largest turbulent motions are almost as large as the characteristic width of the flow, consequently are directly affected by the boundary geometry and hence are not universal. There are a large range of timescales and length scales. The wide spectrum of the relevant scales of the turbulent is a consequence of the nonlinear terms of the conservation equations. Turbulence is regarded as the

Figure 1-2 Sketch of Leonardo da Vinci

Figure 1-1 Leonardo da Vinci (1452-1519), his drawing and statement of coherent vortices around piers (The Royal Library, Windsor Castle)

main unresolved problem in "classical physics". This was also illustrated by Leorando da Vinci (1452-1519) by his description of turbulent flow in his drawing in the fifteenth century. As shown in Figure 1, Leonardo da Vinci gave the following description: "The clouds scattered and torn, Sand blown up from the seashore, Trees and plants must bend". Until nineteenth century, no mathematical model was available to describe viscous flow. Technically turbulence can not be treated just by solving basic equations of fluid mechanics. To achieve simulation of turbulence, various models are introduced. Understanding the physics of turbulence would pave the way to the development of reliable models. There are a variety of approaches for resolving the phenomena of fluid turbulence. The most direct approach is direct numerical simulation (DNS) which solves the Navier-Stokes equations on a mesh that is fine enough to resolve all length scales in turbulent flow. Unfortunately, direct numerical simulation is limited to simple geometries and low-Reynolds number flows because of the limited capacity of even the most sophisticated supercomputers. Alternatives are large eddy simulation (LES) and the Reynolds-averaged Navier-Stokes (RANS) equations. LES solves the Navier-Stokes equations in conjunction with a subgrid turbulence model. The RANS equations are derived by decomposing the velocity into mean and fluctuating components. Figure 2 presents the basic concept of turbulence modeling.

2.2.1 Direct Numerical Simulation

It is possible to directly solve the Navier-Stokes equations for laminar flow cases and for turbulent flows when all the relevant length scales can be contained on the grid. This solution approach of resolving all the scales is known as Direct Numerical Simulation (DNS). Because all the length and time scales have to be resolved. DNS is computationally expensive. In general, the range of length scales appropriate for flows of practical importance is larger than even today's massive supercomputers can model. DNS approach is restricted to flows with low-to-moderate Reynolds number. To resolve the smallest scale of turbulence, a number of grids proportional to $Re^{9/4}$ is required, where Re is the Reynolds number [5]. As an example, for a feasible case of $Re \sim 10^4$, a domain of about 10^9 meshes is acquired. Even with the expected advances in computers, the cost of such simulation will remain easily inaccessible for a long time. Recently, DNS are being used for small scale investigation for better understanding the basic mechanisms of certain physical phenomena.

2.2.2 Reynolds-averaged Navier Stokes equations (RANS)

The Reynolds averaged Navier-Stokes equations (RANS) are obtained by ensemble average of the conservation equations which introduces new apparent stresses known as Reynolds stress. Various

models are developed to provide different levels of closure [6]. RANS models can be divided into two broad approaches. The first is known as Bousinesq hypothesis which uses algebraic equations for estimating the Reynolds stresses which include the turbulent viscosity, and depending on the level of sophistication of the model. This may involve solving transport equations for evaluating the turbulent kinetic energy and dissipation. Models include κ-ε, , κ–ω, Mixing Length Model and Zero Equation. The models in this approach are referred to by the number of transport equations they include. For example, Mixing Length model is a "zero equation" model since no transport equations are solved. However, the K-ε on the other hand is a "two equation" model because two transport equations are solved.

The second approach is known as Reynolds stresses model (RSM) which solve transport equations for the Reynolds stresses. This approach needs more CPU than the Bousinesq hypothesis.

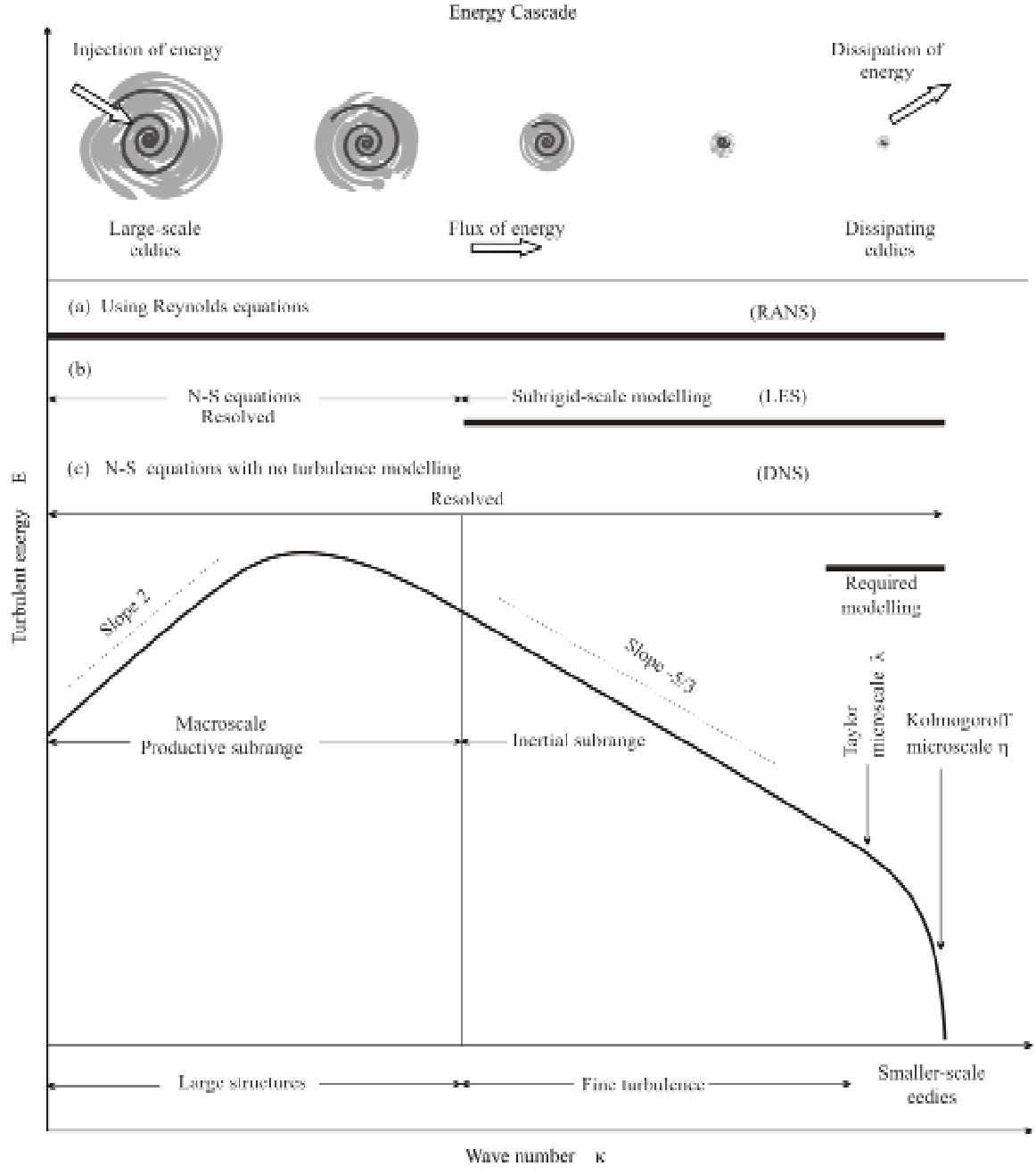

Figure 2 Turbulence model concepts

2.2.3 Large Eddy Simulation (LES)

In LES, the smaller eddies are filtered and are modeled using a subgrid model while the larger energy carrying eddies are simulated. This method requires more a refined mesh that the RANS model. The underling premise is that the largest eddies are directly effected by the boundary conditions and should be computed. By contrast, the small-scale turbulence far from the wall is more nearly isotropic and has universal characteristics; it is thus more amenable to modeling. Figure 2 presents the basic concepts of the LES modeling. The principal advantage of LES over DNS is the fact that it allows to compute flows at Reynolds numbers much higher than those feasible in DNS. In fact, given sufficiently fine resolution, LES approaches direct numerical simulation (DNS) whose accuracy is large.

As illustrated in Figure 2, the center of the wave number range of the spectra exhibits power-law behavior of 5/3 which is the inertial subrange. Low wave number represents the energy-containing range. At high wave number, spectra decay rapidly which is representing the dissipation range.

Subgrid modeling

The Navier-Stokes equations are filtered resulting into equations for the large scale component of the velocity contain terms representing the effect of small scales on the large ones [5, 7-9]. These subgrid (SGS) Reynolds Stresses should be modeled. When the SGS Reynolds stress is a small part of the total time-averaged turbulence, the results produced by LES are relatively insensitive to the quality of the model. The choice of model and values of parameters are of only moderate importance. On the other hand, when LES is applied to complex and or high Reynolds number flows, much of the Reynolds stresses lies in the unresolved scales and model quality becomes more important. The details of subgrid models can be obtained from references 5, 7-9, among others (Pope, 2000; Barsamian, 2000; Hassan, et al., 2001; 2004).

The non filtered Navier Stokes equations for incompressible flows can be represented as:

$$\frac{\partial u_i}{\partial t} + \frac{\partial u_i u_j}{\partial x_j} = -\frac{1}{\rho}\frac{\partial p}{\partial x_j} + \frac{\mu}{\rho}\frac{\partial^2 u_i}{\partial x_j \partial x_j} \qquad (4)$$

in which the Einstein's convection of summation over repeated indices are adopted. Prior to performing large eddy simulation, the governing equations are spatially filtered to remove motions at length (and time) scales not resolvable on the computational mesh. Thus only the "large eddies" are simulated. The flow variable can be decomposed into a large scale (resolved) and a small scale (unresolved) parts and any flow variable *f* can be written such as:

$$f = \overline{f} + f'$$

where $\overline{f}$, the large scale part and is defined through volume averaging as:

$$\overline{f}(x_i, t) = \int_{Vol} G(x_i - x_i') f(x_i - x_i') dx_i$$

where $G(x_i - x_i')$ is the filter function (It can be box filter, Gaussian filter, etc.).

After performing the volume averaging, the filtered Navier Stokes equations become:

$$\frac{\partial \overline{u_i}}{\partial t} + \frac{\partial \overline{u_i u_j}}{\partial x_j} = -\frac{1}{\rho}\frac{\partial \overline{p}}{\partial x_i} + \frac{\mu}{\rho}\frac{\partial^2 \overline{u_i}}{\partial x_j \partial x_j} \quad (5)$$

the over bar denotes the application of the spatial filter. The non linear transport term in the filtered equation can be expressed as:

$$\overline{u_i u_j} = \overline{(\overline{u_i} - u_i')(\overline{u_j} - u_j')}$$
$$= \overline{\overline{u}_i \overline{u}_j} + \overline{\overline{u}_i u_j'} + \overline{\overline{u}_j u_i'} + \overline{u_i' u_j'}$$

(1) (2) (3) (4)

In time averaging, the terms (2) and (3) vanish, but when using volume averaging this is no longer valid. Introducing the sub-grid scale (SGS) stresses, τ_{ij} , as:

$$\tau_{ij} = \overline{u_i u_j} - \overline{u}_i \overline{u}_i$$

The filtered Navier Stokes equations can be written as:

$$\frac{\partial \overline{u_i}}{\partial t} + \frac{\partial \left(\tau_{ij} + \overline{u}_i \overline{u}_j\right)}{\partial x_j} = -\frac{1}{\rho}\frac{\partial \overline{p}}{\partial x_i} + \frac{\mu}{\rho}\frac{\partial^2 \overline{u_i}}{\partial x_j \partial x_j} \quad (6)$$

$$\frac{\partial \overline{u_i}}{\partial t} + \frac{\partial (\overline{u}_i \overline{u}_j)}{\partial x_j} = -\frac{1}{\rho}\frac{\partial \overline{p}}{\partial x_i} + \frac{\mu}{\rho}\frac{\partial^2 \overline{u_i}}{\partial x_j \partial x_j} - \frac{\partial \tau_{ij}}{\partial x_j} \quad (7)$$

where,

$$\tau_{ij} = \overline{u_i u_j} - \overline{u}_i \overline{u}_j = \overline{\overline{u}_i \overline{u}_j} + \overline{\overline{u}_i u_j'} + \overline{\overline{u}_j u_i'} + \overline{u_i' u_j'} - \overline{u}_i \overline{u}_j$$
$$= L_{ij} + C_{ij} + R_{ij} \quad (8)$$

and,

$L_{ij} = \overline{\overline{u}_i \overline{u}_i} - \overline{u}_i \overline{u}_i$ Leonard Stresses

$C_{ij} = \overline{\overline{u}_i u_j'} + \overline{\overline{u}_j u_i'}$ Cross Term

$R_{ij} = \overline{u_i' u_j'}$ SGS Reynolds Stresses

Leonard (1974) showed that the Leonard stress term removes significant energy from the resolvable scales [10]. It can be computed directly and does not need be modeled. The cross-term stress tensor C_{ij} also drains significant energy from the resolvable scales. Current efforts are to model the sum C_{ij} and R_{ij} . Clearly, the accuracy of a LES depends upon the model used for these terms.

Smagorinsky model

The Smagorinsky model can be thought of as combining the Reynolds averaging assumptions given by $L_{ij} + C_{ij} = 0$ with a mixing-length based eddy viscosity model for the Reynolds SGS tensor [11]. It is thereby assumed that the SGS stresses are proportional to the modulus of the strain rate tensor, $\left|\overline{S}_{ij}\right|$, of the filtered large-scale flow:

$$\tau_{ij} - \frac{1}{3}\tau_{kk} = -2 \cdot \upsilon_{SGS} \cdot \overline{S_{ij}} = \upsilon_{SGS} \cdot \left| \frac{\partial \overline{u_i}}{\partial x_j} + \frac{\partial \overline{u_j}}{\partial x_i} \right| \quad (9)$$

To close the equation, a model for the SGS viscosity υ_{SGS} is assumed. Based on dimensional analysis the SGS viscosity can be expressed as:

$$\upsilon_{SGS} \propto l q_{SGS}$$

where *l* is the length scale of the unresolved motion (usually the grid size $\Delta = (Vol)^{1/3}$ and q_{SGS} is the velocity of the unresolved motion.

In the Smagorinsky model which is based on an analogy to the Prandtl mixing length model, the velocity scale is related to the gradients of the filtered velocity:

$$q_{SGS} = \Delta \left| \overline{S} \right|$$

where

$$\left| \overline{S} \right| = \left(2\overline{S_{ij} S_{ij}} \right)^{1/2}$$

This yields the Smagorinsky model for the SGS viscosity:

$$\upsilon_{SGS} = (C_S \Delta)^2 \left| \overline{S} \right|$$

with C_S the Smagorinsky constant. The value of the Smagorinsky constant for isotropic turbulence with inertial range spectrum is:

$$E(k) = C_k \varepsilon^{2/3} k^{-5/3}$$

$$C_S = \frac{1}{\pi} \left(\frac{2}{3C_k} \right)^{3/4} = 0.18$$

For practical calculations the value of C_S is changed depending on the type of flow. Its value is found to vary between a value of 0.065 (channel flows) and 0.25. Often a value of 0.1 is used. In fact, the coefficient C_S varies in space and time.

Dynamic model

To overcome the difficulty of estimating C_S dynamic model can be utilized (Germano et al 1991; Barsamian 2000). In the dynamic model a procedure is used that allows for the estimation of the Smagorinsky constant from the instantaneous resolved flow [12]. A second filter of width larger than the first filter is applied to equation 4. An expression from the two filtered results would provide the estimation of Smagorinsky coefficient. Further details of this model are available in the references mentioned above. The coefficient expression varies strongly in space and time and may contain a fraction of negative values. Consequently, Barsamian has to adopt an averaging procedure to achieve un-oscillatory values of C_S and to remove the local indeterminacy attached to the expression. However, it is important to note that this model has a number of features that make it attractive for complex transitional and turbulent flow. These include (*a*) no *ad hoc* specification of model constants; (*b*) no requirement for a wall model; (*c*) automatic detection of laminar and turbulent regions which is important in the computation for natural circulation phenomena; and (*d*) capability to predict transition to turbulence. The last two are especially attractive for pulsatile and oscillating flows and also when the flow switching between states of stagnation and flowing since, first, these flows constantly cycle between laminar and turbulent states, and second, a capability for *predicting* the onset of turbulence obviates the need for any *ad hoc* assumptions regarding the transition process. These features are delineated during natural circulation flows.

Recently, numbers of dynamic model derivatives such as dynamic mixed models have been proposed. LES requires considerable computing efforts, especially when it is applied to spatially developing flows, which require millions of grid points and long averaging times to achieve convergence of the statistics. It is, therefore, imperative that the dynamic subgrid models do not increase the cost of calculation. The CPU time used by dynamic eddy viscosity model requires a small amount of the total CPU, only ~ 7% more than the Smagorinsky model. More complex dynamic models may require substantial amount of CPU time. For example, two-coefficient dynamic models require over 30% of the CPU time only to model evaluation.

2.2.4 Detached Eddy Simulations (DES)

Detached-Eddy Simulation (DES) is a hybrid technique, first proposed by Spalart et al. (1997), for prediction of turbulence flows at high Reynolds number [13, 14]. DES is a modification of a RANS model in which the model switches to a subgrid scale formulation in regions fine enough for LES calculations. Regions near solid boundaries and where the turbulent length scale is less than maximum grid dimension are assigned the RANS mode of solution. As the turbulent scale exceeds the grid dimension, the regions are solved using LES mode. Therefore the grid resolution is not as demanding as conventional LES; consequently, affordable CPU time is consumed. The switching between RANS and LES models is made at a suitably chosen interface. The key problem is to ensure proper matching conditions at the interface.

3. METHODOLGY AND SOLUTION TECHNIQUES

In all these modeling approaches the same basic procedure is followed:

1. The geometry (physical bounds) of the problem is defined.
2. The volume occupied by the fluid is divided into discrete cells (mesh). The mesh may be uniform or non uniform, structured or unstructured mesh.
3. The physical modeling is defined; i.e. the conservation equations
4. Boundary conditions are defined. This involves specifying the fluid behavior and properties at the boundaries. For transient problems, the initial conditions are also defined.
5. The equations are solved iteratively
6. Analysis and visualization of results

Boundary conditions for DNS and LES are one of the most important issues. Boundary conditions can be grouped into several classes:

- *Periodic boundary conditions*, which can be used in directions of statistical homogeneity of the flow. The size of the domain must be chosen so that fluctuations can not spuriously interact with themselves through periodic boundaries.
- *Outflow boundary conditions*, which must be designed to prevent spurious reflextions on the boundary.
- *Wall boundary conditions*, in case the no-slip condition associated to the wall is not relevant, because scales of motion in the very near wall region are not captured. As a consequence, a specific subgrid model for the inner layer, referred as a wall model, must be defined, which should provide the simulation with adequate conditions on the variables and/or the fluxes.
- *Inflow conditions*, the main problem arises when the incoming flow is turbulent, because all the resolved scales of motion should be prescribed at the inlet. This requires a priori a deterministic description of the turbulent flow on the inlet plane. A few existing methods for the inflow velocity field are employed such as, the random method in which the incoming velocity is split to stationary and fluctuating part. The stationary part is assumed to be known from experiments, RANS simulations or theory, while the fluctuating part is defined as a random function.

3.1 Discretization Methods

The following are different methods are being used in several CFD codes:

Finite difference method

This method has historical importance and is simple to program. The numerical solution of partial differential equations (PDEs) requires first the discretization of the equations to replace the continuous differential equations with a system of simultaneous algebraic difference equations [15]. The construction of the solution process involves representing the difference equation at discrete points. It involves replacing the partial (or ordinary) derivatives with a suitable algebraic difference formulation. This is accomplished by performing Taylor series expansions of the solution variables at several neighbors of the points of evaluation, which amounts to taking the solution to be represented by polynomials between points. This can be unrealistic if the result varies too sharply between points. One remedy is to use more points so that the spacing between points is reduced. However, a uniformly fine grid is very expensive as numerous points will be wasted in regions of small variation. An alternative approach is to make the points unequally spaced; i.e., the use of nonuniform grids. This indicates that accurate resolution of the solution requires that grid points be clustered in the zones of large gradients and be spread out in regions of small gradients

Finite volume method

This is a standard approach used in most commercial software. The governing equations are solved on discrete control volume. This integral approach yields a method that is inherently conservative. Several commercial CFD codes use this approach in the approximation of the conservation equations.

Finite element method

This method is popular for structural analysis, but is also applicable for fluids. The finite element formulation requires special care to ensure a conservative solution. In this method a weighted residual equation is formed.

Boundary element method

The boundary occupied by the fluid is divided into surface mesh. The major motivation behind boundary element method is to reduce the dependency of the analysis on the definition of meshes. This has allowed the method to expand naturally to new techniques such as mesh reduction method.

Spectral Method

This method can be viewed as semi-analytical alternatives to finite differences for spatial differentiation in application where high degree of accuracy is required. These methods are also referred to as transform methods. Fourier transform and Chebyshev polynomial expansions are examples of these transform expansions.

3.2 Solution Techniques

The basic solution of the system of equations arising from discretization is accomplished by several algorithms such as Gauss-Seidel, successive overrelaxation, Krylov subspace and multigrid algorithms among others. The solution methods can be for structured, body-fitted coordinates or unstructured grids. Figure 3 presents the simulation and analysis within a CFD environment.

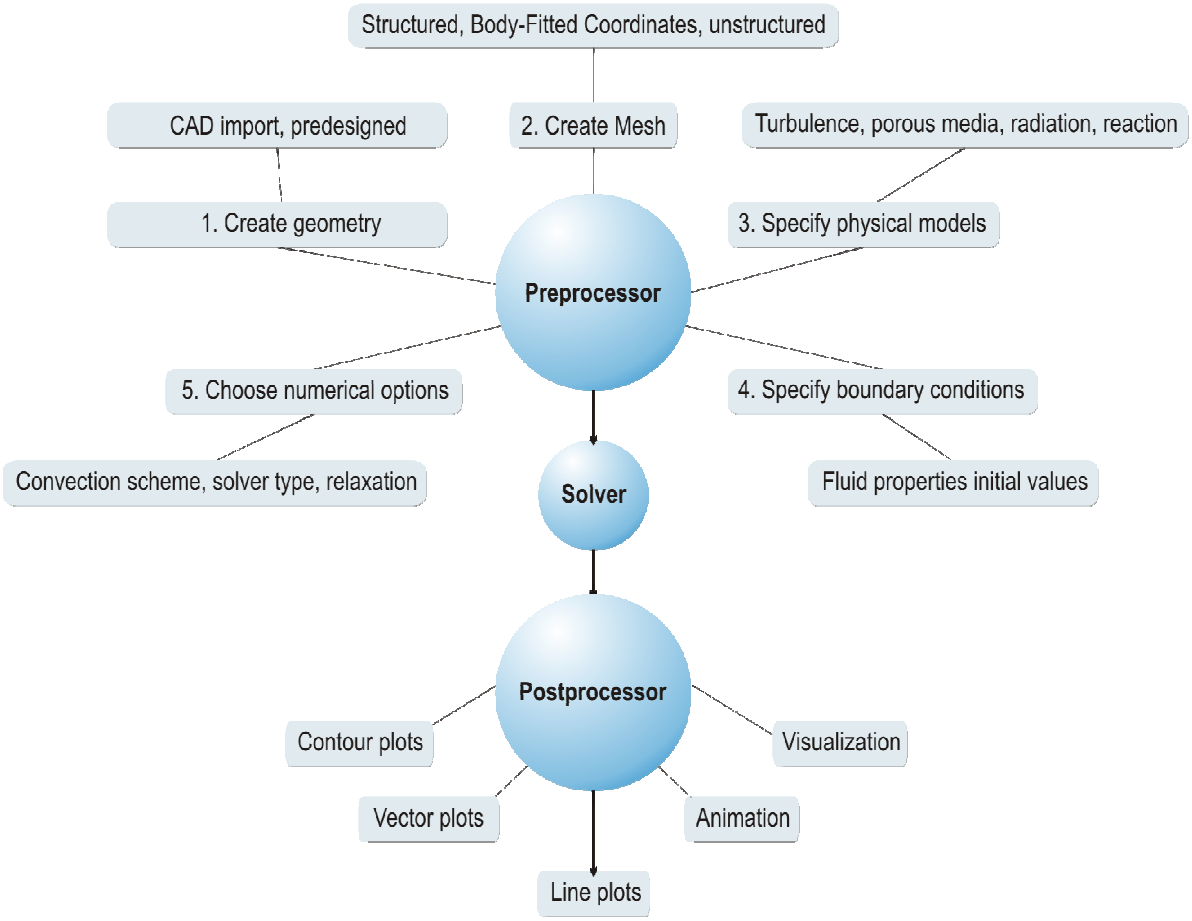

Figure 3 The simulation and analysis tools for CFD

4. CFD IN NATURAL CIRCULATION AND NUCLEAR APPLICATIONS

For some specific applications it was found necessary to use CFD tools to be able to zoom on a portion of the circuit where physical phenomena are important for safety issues and design optimization. The principal interest of computational fluid dynamics (CFD) in nuclear applications is mainly in the capability to obtain at a lower cost, valuable information on some physical phenomena. Accurate numerical simulations would aid to test any configuration, from both qualitative and quantitative points of view, and thus to evaluate and/or discriminate different designs according to pre-determined criteria. These criteria may be linked to economical or technological constraints, and/or to safety and environmental issues. Concerning safety issues in the nuclear industry, CFD is being recognized as an important tool in delineating some physical phenomena of the flows. Several commercial codes such as CFX [16], FLUENT [17], STAR-CD [18], among others are being used in reactor safety applications. Also in nuclear community several codes are developed, for example, SATURNE code is developed by EDF and the large eddy simulation single-phase flow TRIO_U code is developed by CEA [19]. A new generation of two-phase flow code covering a whole range of modeling scales for nuclear power plants is being developed by CEA and EDF [20].

It is clear that single-phase flow CFD code solutions for nuclear reactor system applications can have accurate simulations once verification and validation are performed. Here, appropriate turbulence modeling, numerical scheme, nodalization and boundary conditions are also factors in drawing the conclusions of the computations. However, one challenge for single-phase CFD codes that still persists is the modeling of the turbulence in the flow. It has been observed that the turbulence models often do not perform efficiently outside their calibration regime. The flows inside reactor components are rich in turbulent physics, and thus, in author opinion, numerical prediction of these flows is not trivial.

CFD is used for a number of applications in light water nuclear reactors such as:

- Boron dilution;
- Mixing of cold and hot water in the cold legs;
- Heterogeneity in coolant temperature distribution and its effect on pressurized thermal shock (PTS);
- Counter-current flow in cold and hot legs;
- Flows in tee junctions;
- Flow mixing in lower plenum;
- Sump screen debris;
- Fuel element storage tanks;
- Containment flow in loss-of-coolant accident;
- Propagation and mixing of gases (hydrogen, air, steam) in the containment and the effect of gas distribution on the containment dynamics;
- Natural circulations in various reactor components;
- Liquid/gas stratification and interface tracking;
- Bubble dynamics in suppression pools;
- among others.

As illustrated above, CFD have a broad range of applications and provides detailed insight and offer a unique tool for analysis of local phenomena. It is clear that these above topics have tremendous effects once they occur during any phase of the natural circulation scenario. Natural circulation of coolant ensures adequate cooling of the reactor core. It should be known how the circulation flow behaves within the reactor system components under variety conditions. The following sections will illustrate the importance of several CFD calculation needed to study the complex relevant physical phenomena during natural circulation.

Mixing (Pressurized Thermal Shock and Boron Dilution)

Injection of cold water into the cold legs of the primary circuit of a pressurized water reactor (PWR) may lead into incomplete mixing. This may produce thermal loads in the weld of the pressure vessel. The full field of three-dimensional local temperature distributions in cold legs, downcomer annulus, and lower plenum are needed for calculation of thermal shock problem. Also, these temperature distributions are important in driving the natural circulation process. The simulation should be carried out in three-dimensional geometry.

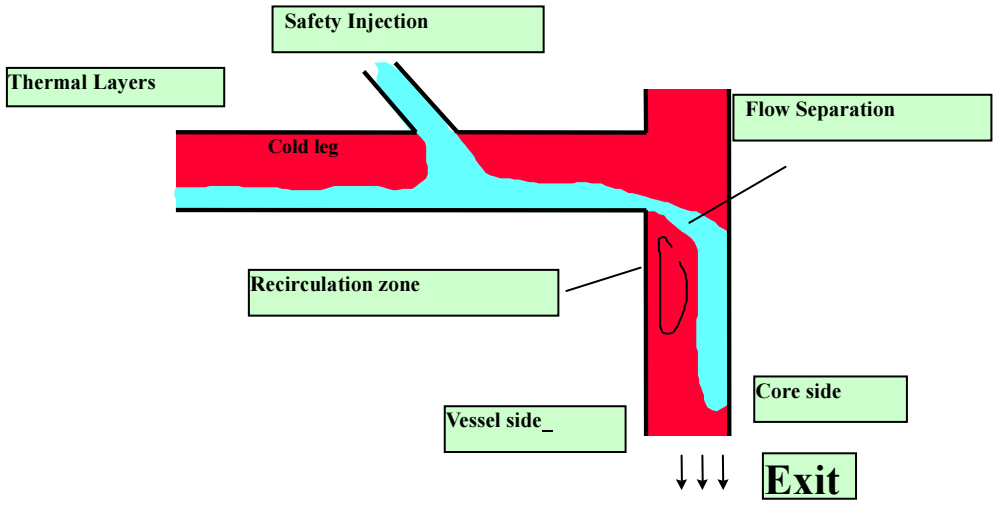

Figure 4 Mixing in cold leg of PWR

Figure 4 presents the complex phenomena in the cold leg with the cold water injection via high pressure injection (HPI) nozzle. Recirculation zone and a distinguish temperature variation are exhibited within the downcomer annulus. Separation and reattachment phenomena are also demonstrated during this scenario.

There may be a potential risk of reactivity excursion accident exist in association with boron dilution events and a poor degree in mixing of diluted fluid in a PWR vessel. For these types of accidents, mixing is a mitigative mechanism against high reactivity insertion, which can lead even to re-criticality of the scrammed reactor. . For boron dilution transients, the diluted slug transport and mixing after reactor coolant pump (RCP) start-up is significant case. The transport of low borated water into the reactor core during re-start of natural circulation after a LOCA might also lead to serious consequences with respect to reactor safety. Here also accurate calculation of mixing is important.

Figure 5 presents three-dimensional CFD temperature calculations in the cold leg and the downcomer. Another detailed modeling all the internals of the reactor vessel of ROCOM mixing test facility in Germany (FZR) facility was performed using CFX code (Hohne, et al, 2005). The pathlines after the buoyancy suppression is shown in Figure 6 [21, 22].

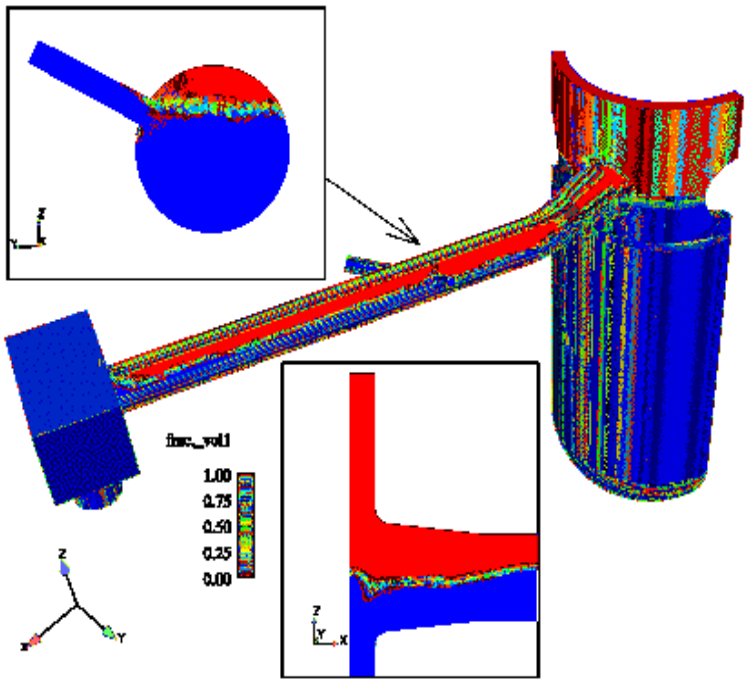

Figure 5 Temperature distributions in the cold leg and downcomer from CFD calculations

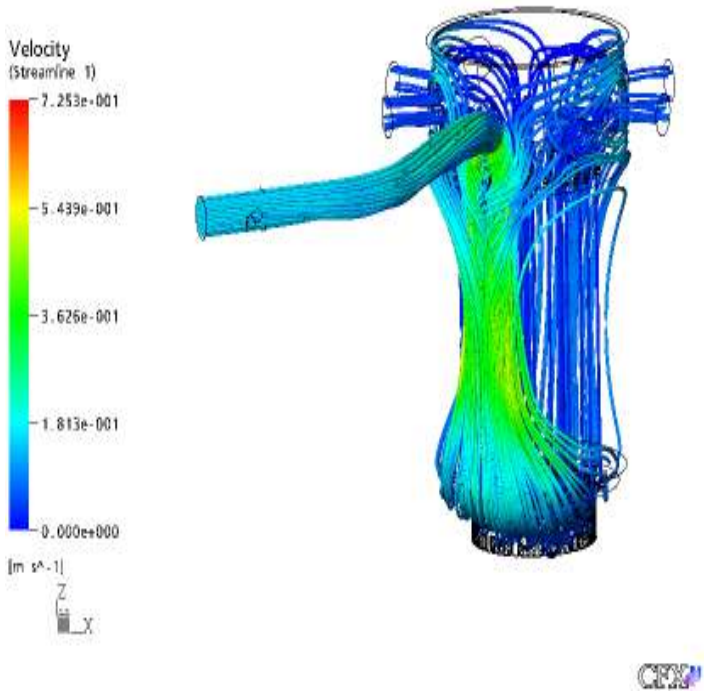

Figure 6 Pathlines of mixing after the buoyancy suppression (time=23 S)

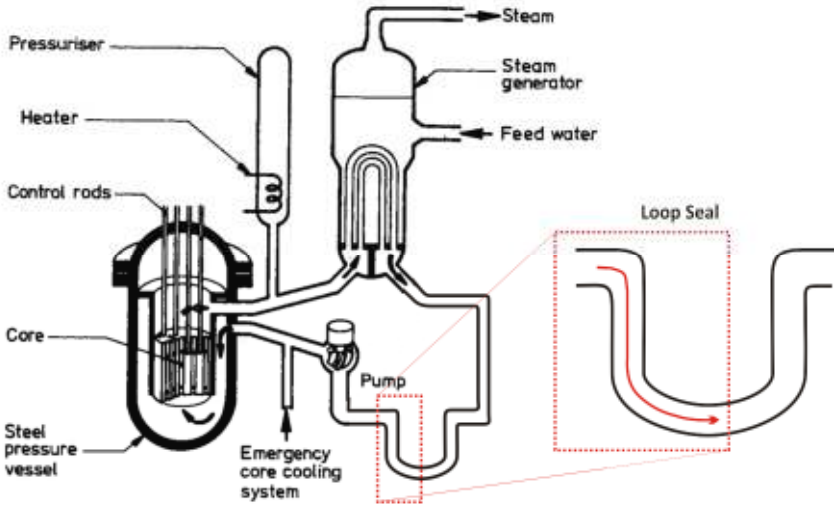

Figure 7 Schematic of PWR with loop seal

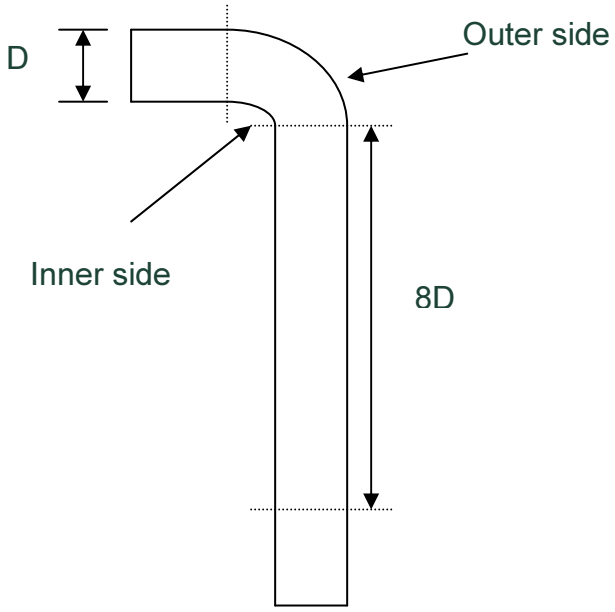

Figure 8 Simulated elbow

The nuclear reactor system contains a large numbers of elbow tubes where the mixing may take place (Figure 7). Under these configurations the velocity distributions are complex and three-dimensional. The mixing features can not be calculated via one-dimensional or thermal-hydraulic system codes. A CFD study is performed for an elbow as a part of the loop seal. The schematic of single elbow geometry is shown in Figure 8. The diameter of the elbow is 0.15 m and the radius of curvature of the elbow is 0.15 m. The Reynolds number of the flow is around 50,000. The tracer gas is

released at the entrance of the elbow [23, 24]. Around 400,000 prismatic cell elements were used for the simulation. The average time step was 5 ms.

The calculations were performed using large eddy simulation (LES) technique. The results from static and dynamic Smagorinsky subgrid scale models are compared. The difference between the static and dynamic subgrid scale model lies in the calculation method for the Smagorinsky constant.

The Smagorinsky constant relates the length scale to the filter width. The characteristic length scale is used to calculate the eddy viscosity from the resolved strain rate magnitude. The static subgrid scale model assumes a uniform Smagorinsky constant throughout the domain, whereas in the dynamic model the Smagorinsky constant is calculated based on the local turbulence characteristics.

Figure 9 presents the LES calculations of the dynamics of tracer injected at the center of the inlet horizontal part of the elbow [23, 24]. A vortex formation and subsequent breakup can be observed from the development of concentration profile. The phenomena of irregular shape of the jet can be explained by the fact that there exist turbulence differences and disturbances between the jet and the ambient fluid. These differences and disturbances would lead to protuberances (swelling and bulging). This feature will affect the subsequent motion and mixing phenomena. These observations are in a good comparison with the experimental visualization results. Down stream of the jet injection in the straight pipe, it is clear that existence of less concentration in the center than its outer part. This reveals existence of a hollow trough. In contrast to the LES results, the conventional K-ε and other RANS models do not reveal this flow structure. To delineate the complex mixing structure, a visualization of a typical steady turbulent plume in a flow obtained when steady state flow conditions have been reached is shown in Figure 10. Evidence for the plume behavior is provided by the lower view. The deflection of the jet or plume toward the crossflow direction results in the development of a counter-rotating vortex system over the cross section of the flow. The lower part of Figure 10 shows that the darker regions associated with the two vortices are separated by a significantly lighter region (less mixing) dominated by the presence of dye-free ambient fluid that is entrained by the vortex system along its plane of symmetry.

Figure 11 presents contours of instantaneous velocity magnitude through mid symmetry plane of the elbow using LES technique. It reveals the complex flow structure at the elbow and downstream of the elbow. This flow patterns computed using LES were different from the RANS calculations. The average flow pattern obtained via LES was also different from RANS result.

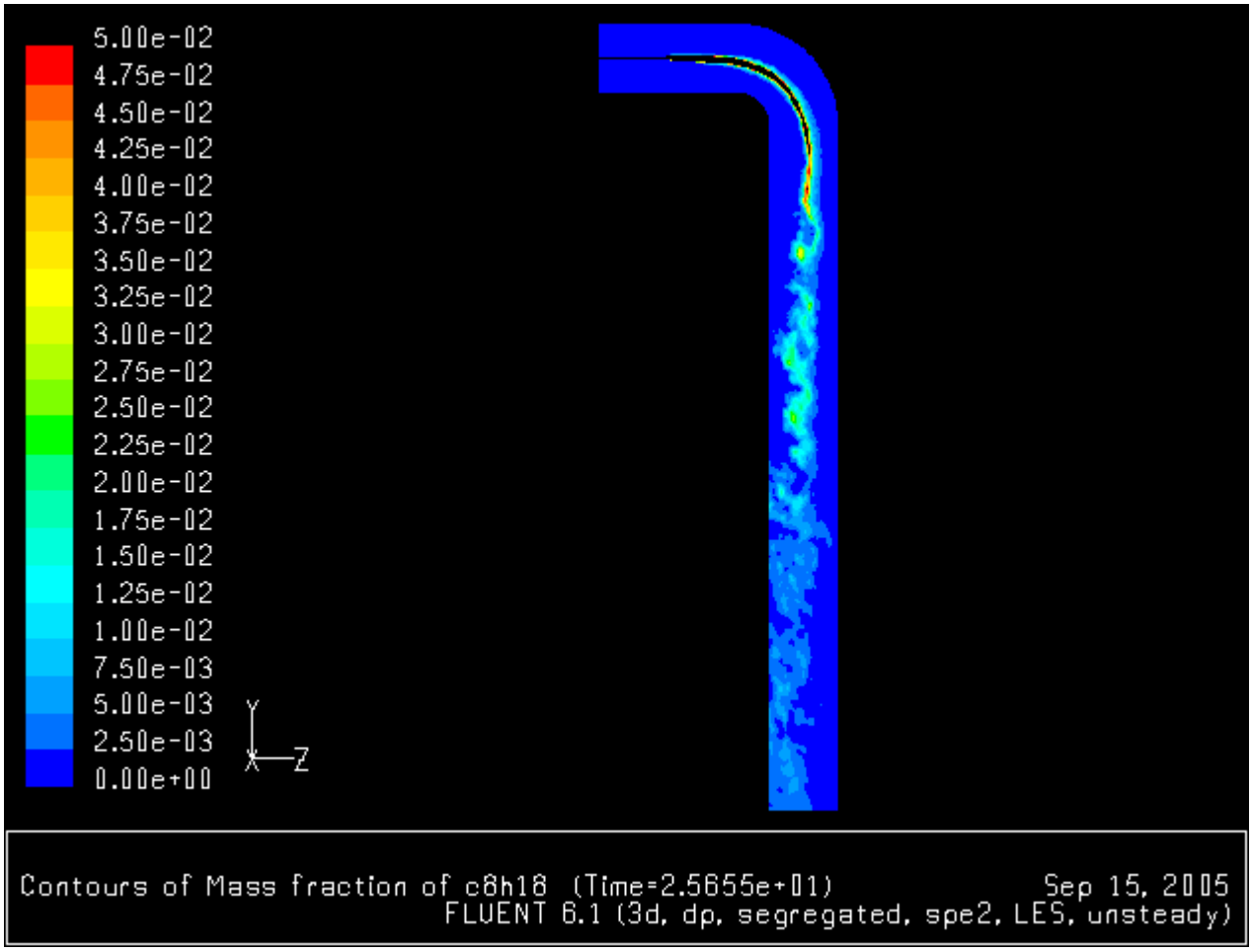

Figure 9 LES Concentration contour dynamic

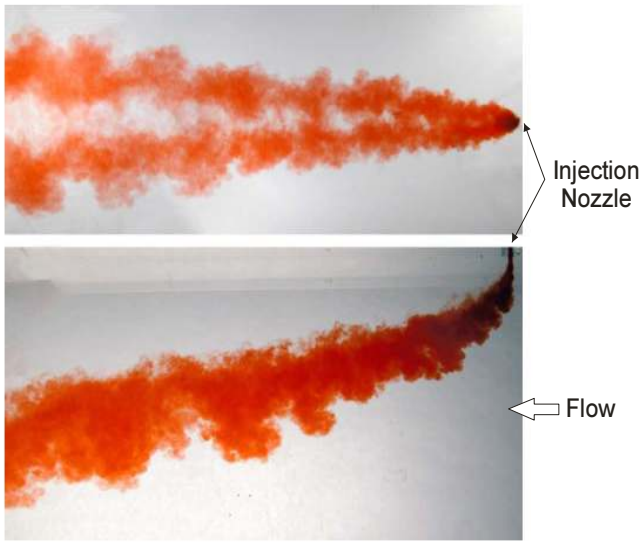

Figure 10 Visualization of the penetration properties of a steady turbulent jet in a uniform crossflow. The upper image shows the top view where as the lower image shows the side view

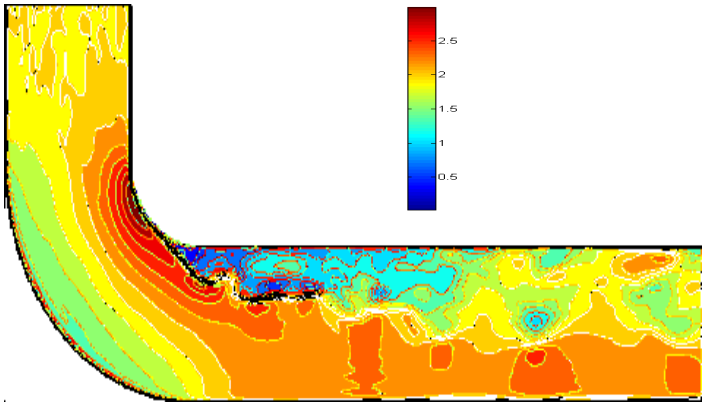

Figure 11 Contours of instantaneous velocity magnitude through mid symmetry plane of the elbow

Figure 12 presents the mean velocity profiles downstream of the elbow using different Reynolds Averaged Navier Stokes (RANS) and Large Eddy Simulation (LES) models to model the turbulence in the flow. The RANS models used for the simulation included standard, realizable, Renormalization Group (RNG) k-ε and the 9- equation Reynolds Stress Models. Static Smagorinsky sub-grid scale model was used for the LES simulations. All the RANS simulations were steady simulations, while by definition the LES simulations were unsteady. It is clear that there is a striking difference of the RANS and LES velocity predictions. There may a little similarity of the velocity profiles for RANS models. However, there is substantial difference between the RANS and LES simulations. The momentum transfer and consequently the dispersion of the tracer gas happen in a toroidal crescent shaped fashion for the RANS simulations. The transport of momentum and tracer gas seems to happen in a much more uniform fashion for the LES simulations in this case. The results of LES simulations compared better with the experimental results. The measure used in the current study for demonstrating the uniformity of momentum or concentration at a cross-section of the flow is the co-efficient of variation (*COV*). *COV* is defined as the standard deviation over the mean for a given set of data points as given in Equation 10.

$$COV = \frac{\sqrt{\frac{1}{N-1}\sum_{i=1}^{N}(x_i - \bar{x})^2}}{\bar{x}} \qquad (10)$$

where :
$\bar{x}$ is the mean
N is the numer of data points

The velocity and tracer gas concentration Coefficient of Variations (*COV*s) were compared with experimental results [23, 24].

The tracer concentration *COV* is shown in Figure 13. It is clear that LES predictions are closer to the experimental values. For example, at a distance of 10 diameters downstream from the exit plane of the single elbow, the concentration COV of 29% predicted using LES is closer to the experimentally predicted value of 20% than the value of 86% predicted using RNG k-ε model. It should be noted that flow separation, flow switching and swirling flows through the 90 degree bends would impact the concentration distribution of species such as Boron.

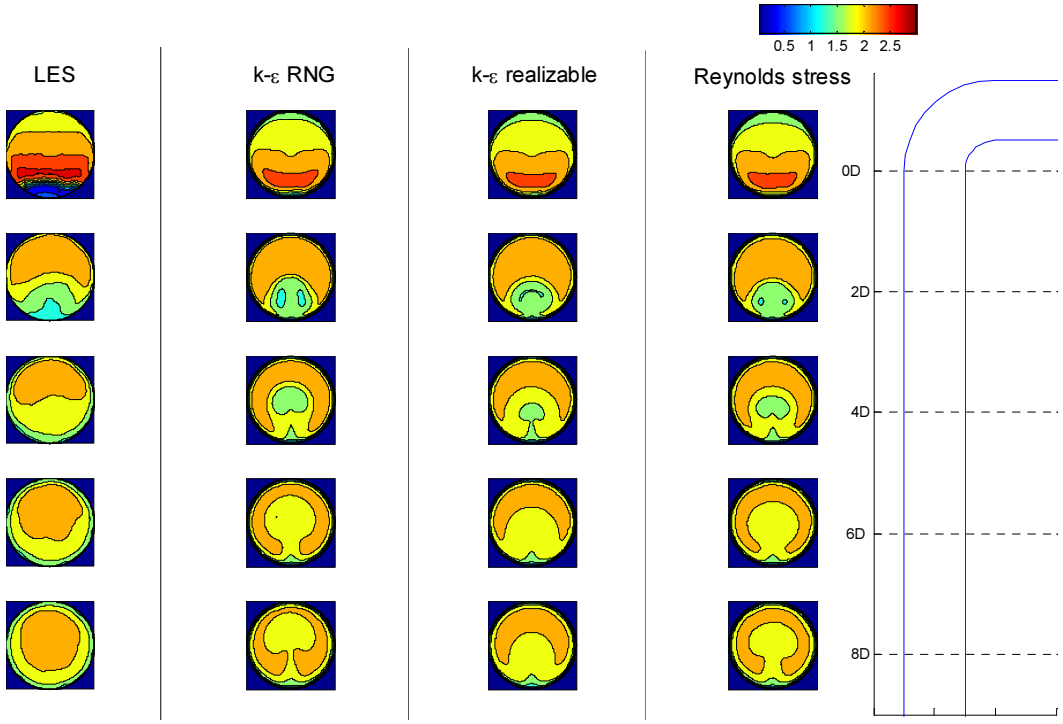

Figure 12 Comparison of the mean velocity profiles through the pipe cross sections at various axial elevations using several turbulence models.

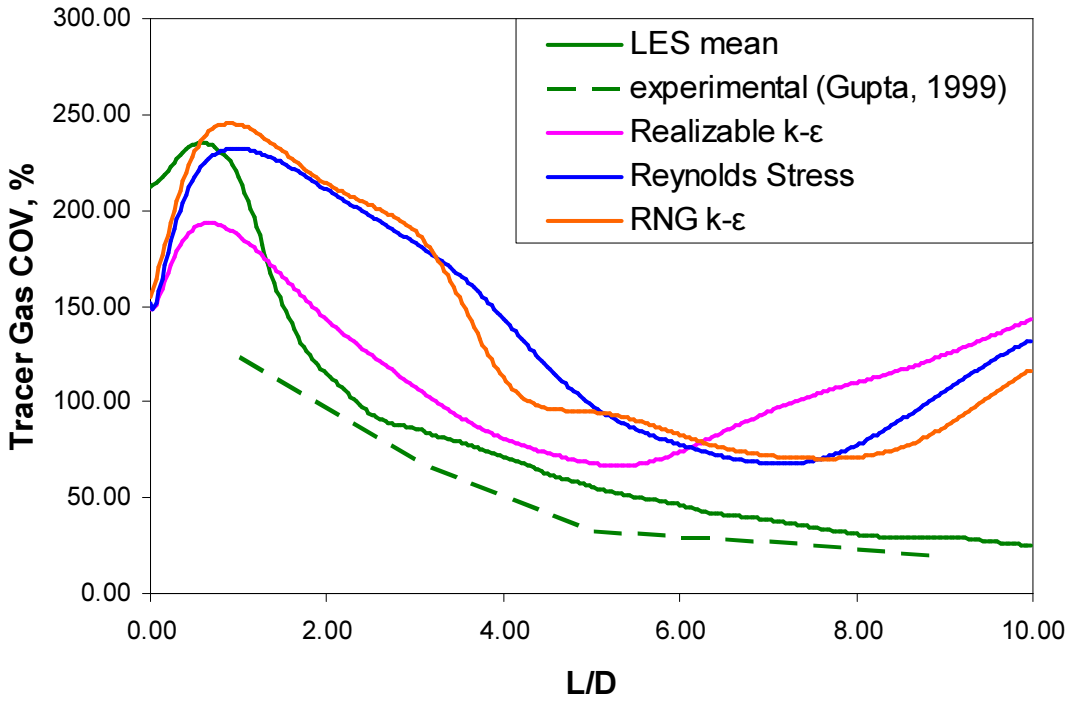

Figure 13 Concentration *COV*s are plotted against the downstream distance from the exit plane of the elbow

Flow in Tee Junctions

In nuclear system there are many Tee junctions where hot and cold fluids are mixed during normal and abnormal operations. This mixing of hot and cold fluids, under certain operating conditions, may result in significant fluctuation or oscillation in the local fluid temperature, commonly referred to as 'thermal striping'. The fluid temperature oscillation can cause high cycle thermal fatigue and even crack damage in the surrounding pipe wall. In addition this mixing will affect the natural circulation phenomena, if it exists. To achieve accurate predictions of the mixing, CFD calculation can be pursued.

A simulation of Tee junction mixing experiment is performed. The condition of the experiment was with main flow temperature of 293 K and the branch flow of 333K [25]. The number of grids was about 100,000. Large eddy simulation was used. Various flow conditions were used branch flow velocities, U_b, of 0.24 m/s, 0.46 m/s, 0.62 m/s with main flow velocity, U_m, of about 0.72 m/s. Figure 14 presents the Tee-junction and the nodalization scheme. Figure 15 presents the temperature and velocity contours for these cases. There are remarkable characteristics in the mixing process at the interface between main pipe flow and branch pipe jet.

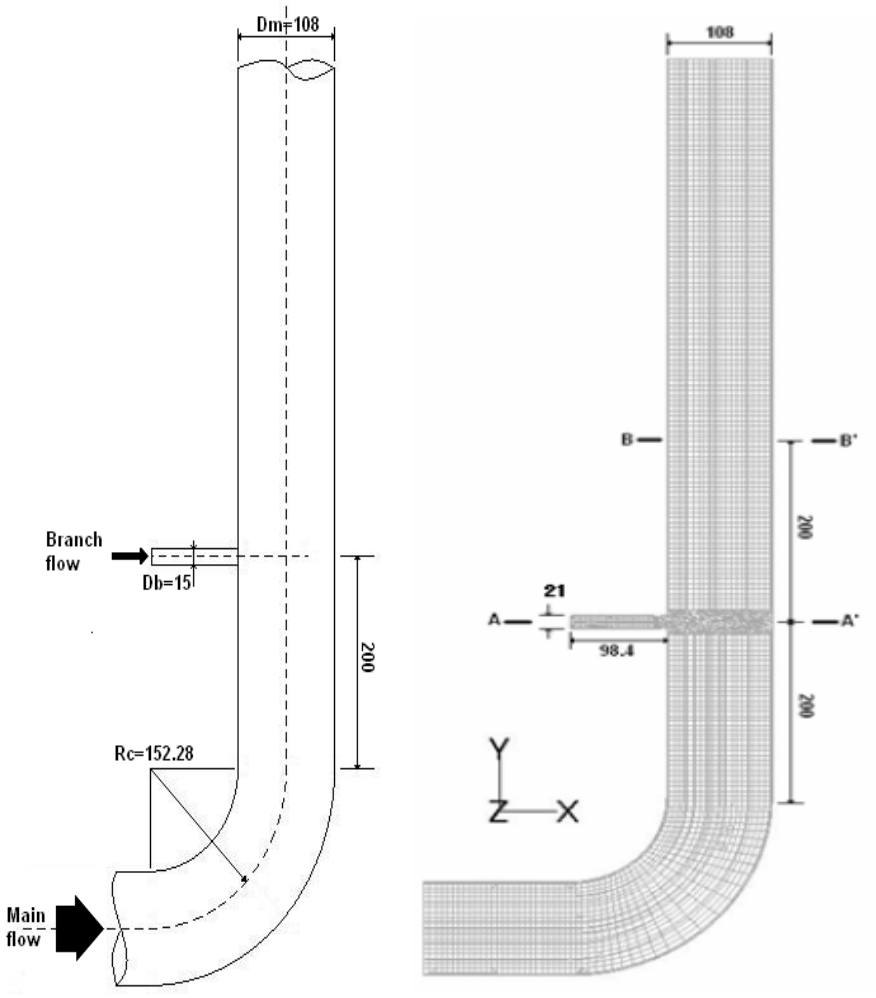

Figure 14 Tee-junction and CFD three-dimensional nodalization scheme

CASE A: Um=0.72 m/s, Ub=0.24 m/s

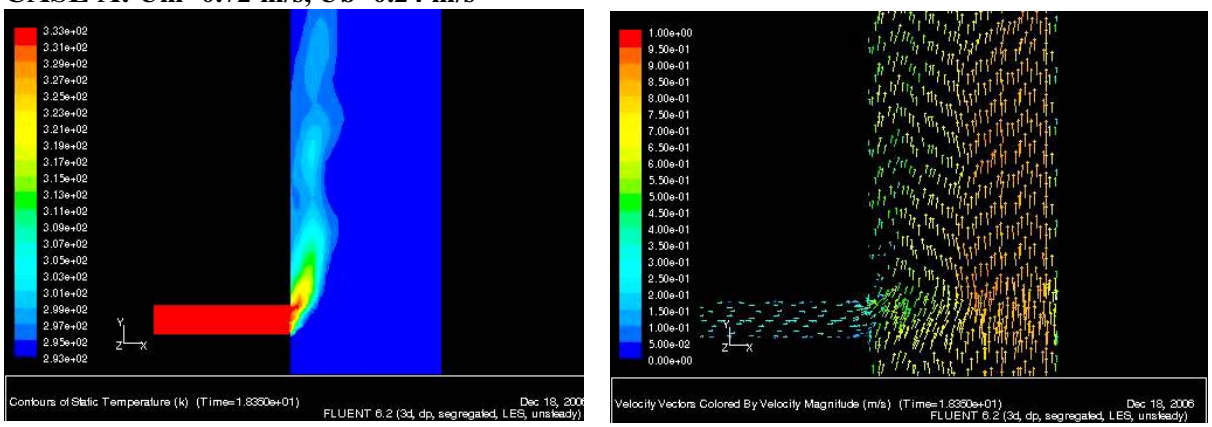

Temperature contour **Velocity Vector**

CASE B: Um=0.72 m/s, Ub=0.46 m/s

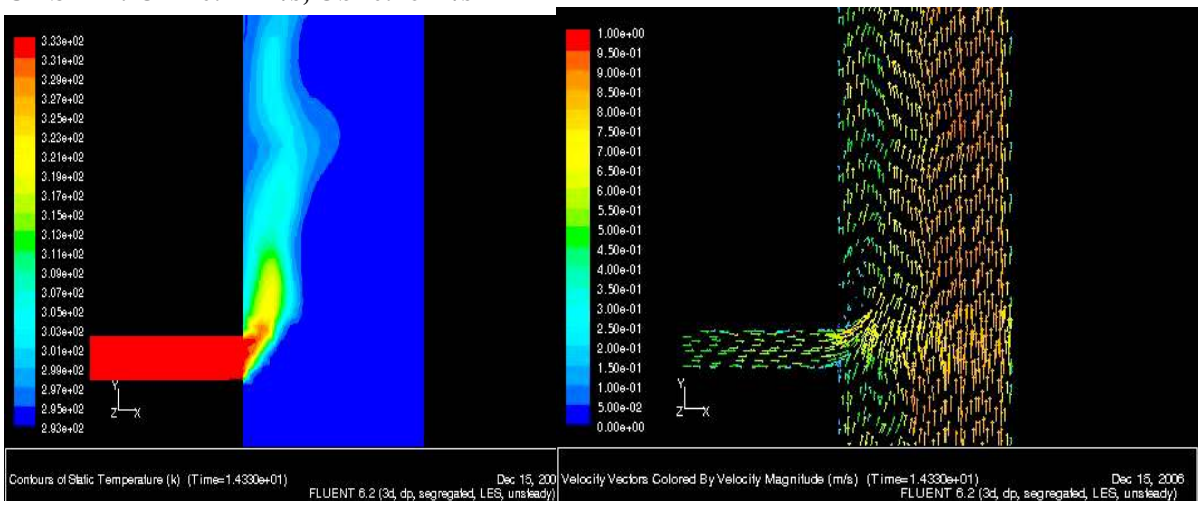

Temperature contour **Velocity Vector**

CASE C: Um=0.72 m/s, Ub=0.72 m/s

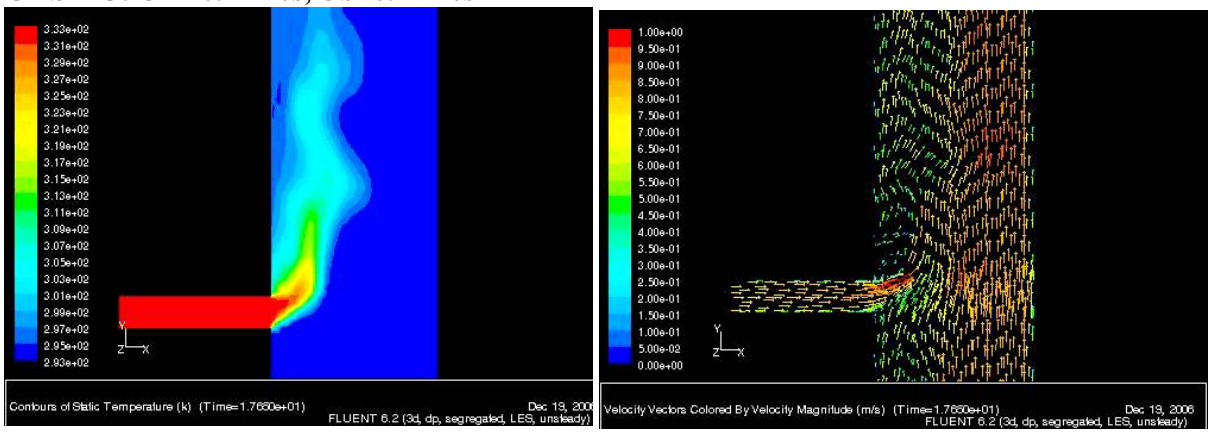

Temperature contour **Velocity Vector**

Figure 15 Temperature and velocity contours in a Tee-junction for various flow rates of the branch section.

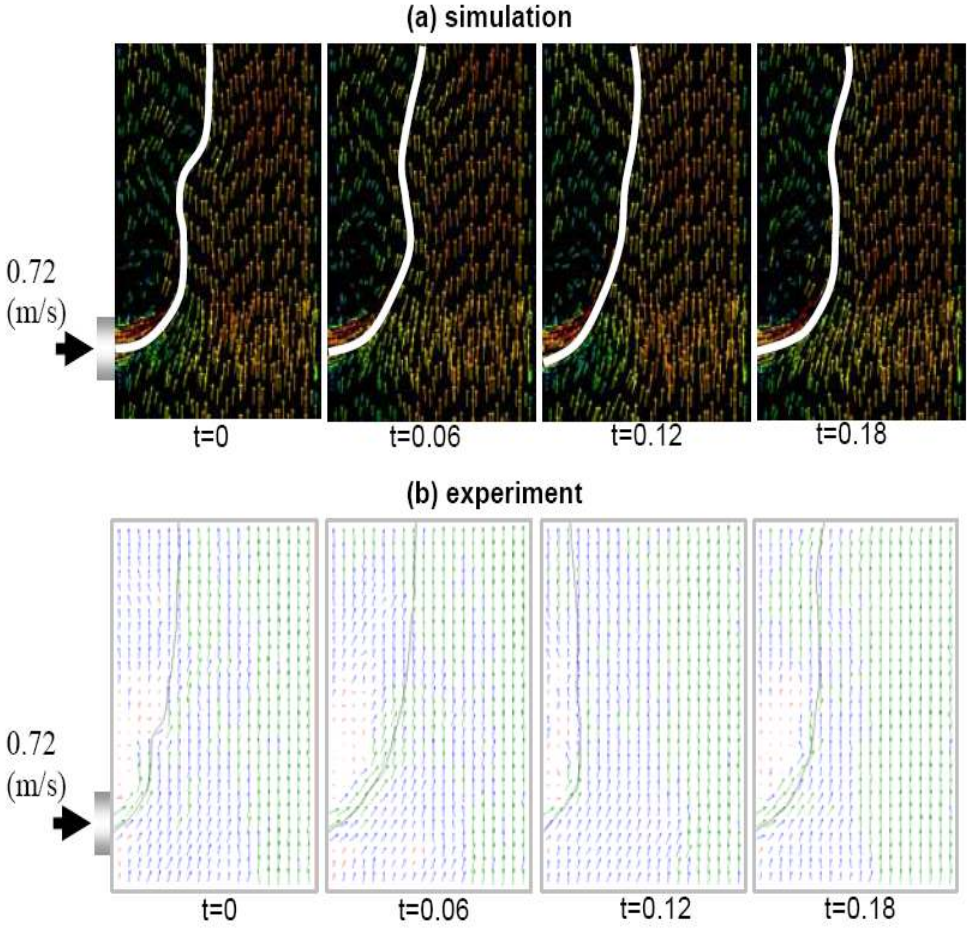

Figure 16 Comparison of the CFD velocity profile prediction with the experimental data for case C. The simulation is the top figure (a), and the experiment is the bottom one (b).

The comparison of the velocity predictions and experimental data are shown in Figure 16 for case C of equal main and branch flows (0.72 m/s). A reasonable agreement was obtained. Temperature fluctuation near a surface along the flow direction is presented in Figure 17. The color delineates the intensity of temperature fluctuations. It is clear that with case A (Ub=0.24 m/s) a strong temperature fluctuations are obtained near the branch surface.

Many of failures caused by wall thinning (metal loss) in carbon steel piping systems/components have been experienced worldwide and occurred in most of types of nuclear power plants. It has been well known that such wall thinning has been caused by the flow-accelerated corrosion (FAC), one of the mechanical chemical degradation mechanisms affecting the integrity of piping systems/components. Especially, intensive studies to understand the parameters affecting FAC have been initiated since Surry unit 2 wall thinning failure in 1986 (see Figure 18), and then many regulatory technologies have been developed to guarantee the integrity of piping systems/ components since the accident occurrence [26, 27]. It is indicated that the shear stress and velocity gradient at the pipes connection is a dominant factor affecting FAC which causes local wall thinning.

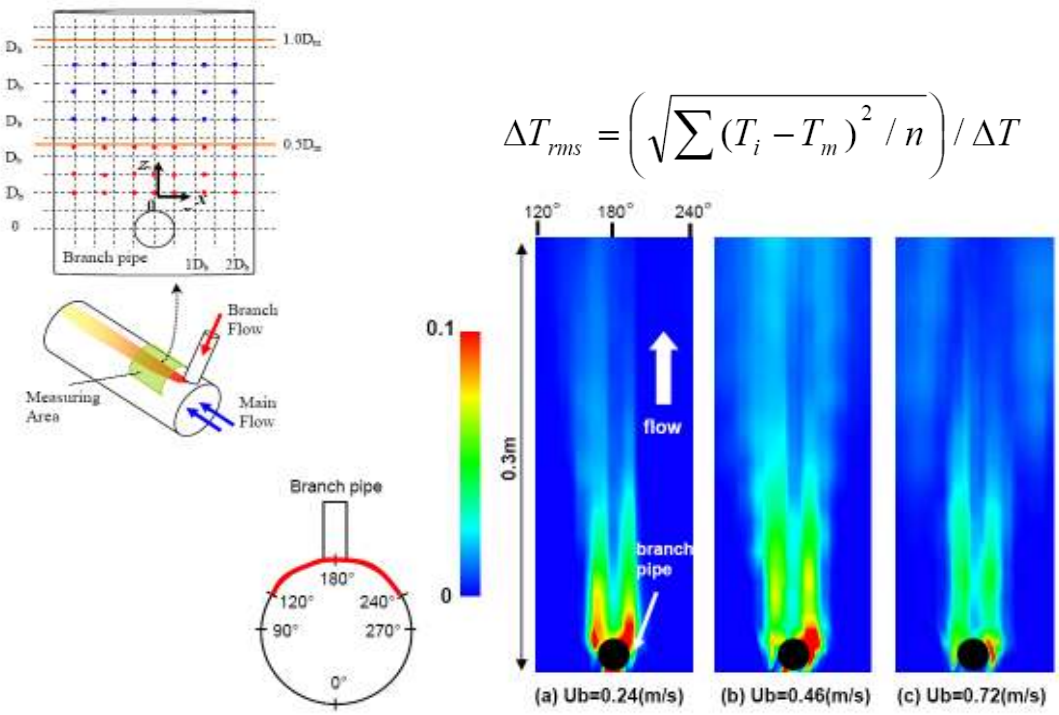

$$\Delta T_{rms} = \left(\sqrt{\sum (T_i - T_m)^2 / n} \right) / \Delta T$$

Figure 17 Fluctuation temperature intensities predictions

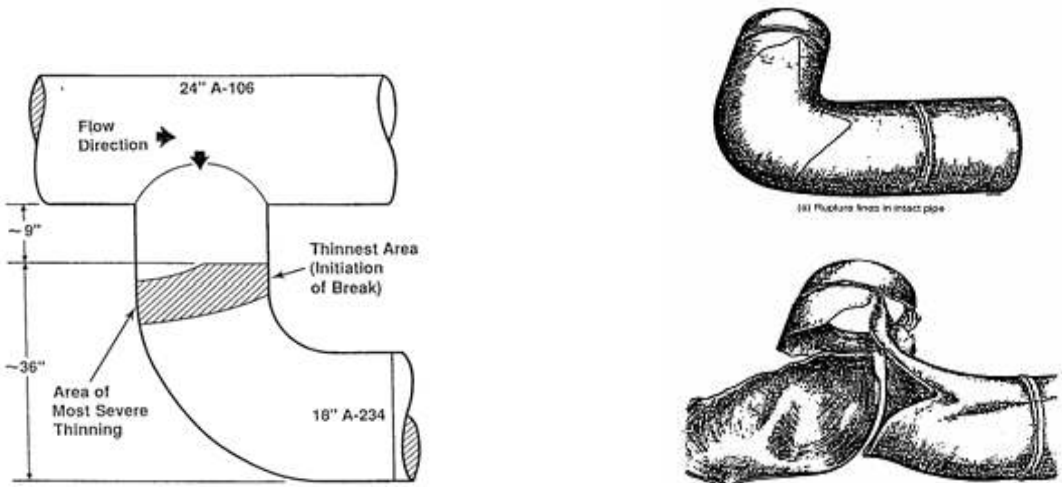

Figure 18 Schematic result of Surry unit 2 wall thinning

Mixing of Jet Flow in Rod Bundle

In nuclear system there are many situations of jet flows. One of the following case for multi-jet flows injected in a rod bundle. There have been numerous studies of flow across single or dual rod configurations with various turbulence model developed, but the present study is concerned with the more complex flow phenomena present in the staggered support rods with cross flows. In this investigation, a model of the fluid domain in the rod bundle was broken into cells across which the characteristic equations of fluid flow (pressure-velocity) could be solved using finite volume discretization and the Semi-Implicit Method for Pressure Linked Equation (SIMPLE) approach. The model under scrutiny (*Figure11*) was geometrically identical to the experimental model employed by Dominquez et al [32] to allow a direct comparison between results. The model has two inlet jets within the bundle, 29 rods staggered in a 3:4 configuration, and one outlet at the end of the channel.

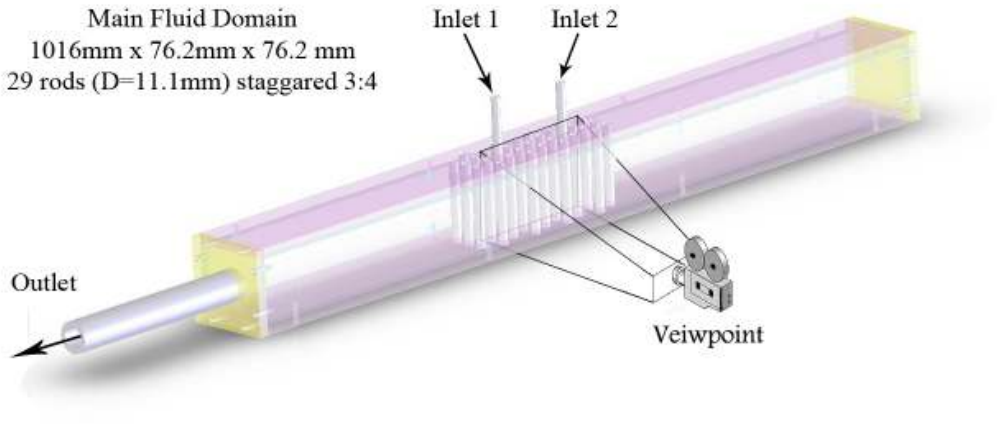

Figure 19 Representation of the model used for numerical simulation.

In the numerical simulation, the two inlets were designated as having Dirichlet boundary conditions with inlet flow velocities to achieve Inlet Reynolds numbers ranged between 4,200 and 12,700. The outlet was specified as having a split-flow boundary condition in which all fluid exited via this sink. Such a treatment was allowed within the Star-CCM+ package[32] since no pressure, stagnation, or mass flow boundary conditions were utilized in development of the numerical model. A length/diameter ratio of 10 was used for the tube length leading to the inlet to ensure that the boundary layer was fully developed prior to flow entering into the bundle array. Under Relaxation factors of 0.2 were used for the velocity, pressure, and turbulence solvers to aid in the convergence of a solution. The solutions of simulations carried out were defined as having reached a converged solution when all residuals reduced to less than 10^{-5}. The development of numerical simulations was conducted in parallel with an experiment using particle image velocity to obtain velocity field by Amini et al [33]. These results were obtained in an effort to evaluate the ability of realizable k-ε turbulence model to reliably predict flow behavior in rod bundles. While computational simulations characterized flow behavior in three-dimensions, planar views are presented to allow direct comparisons of these results with experimental results. In addition to planar views of the velocity profile, line probes of the Y-velocity component are taken along the mid-plane at various heights. The resulting plots allow for a better comparison of how well the turbulence model fit the experimental data. The results are presented in Figures 20 and 21 for single and dual jets along the experimental data from particle image velocimetry[34].

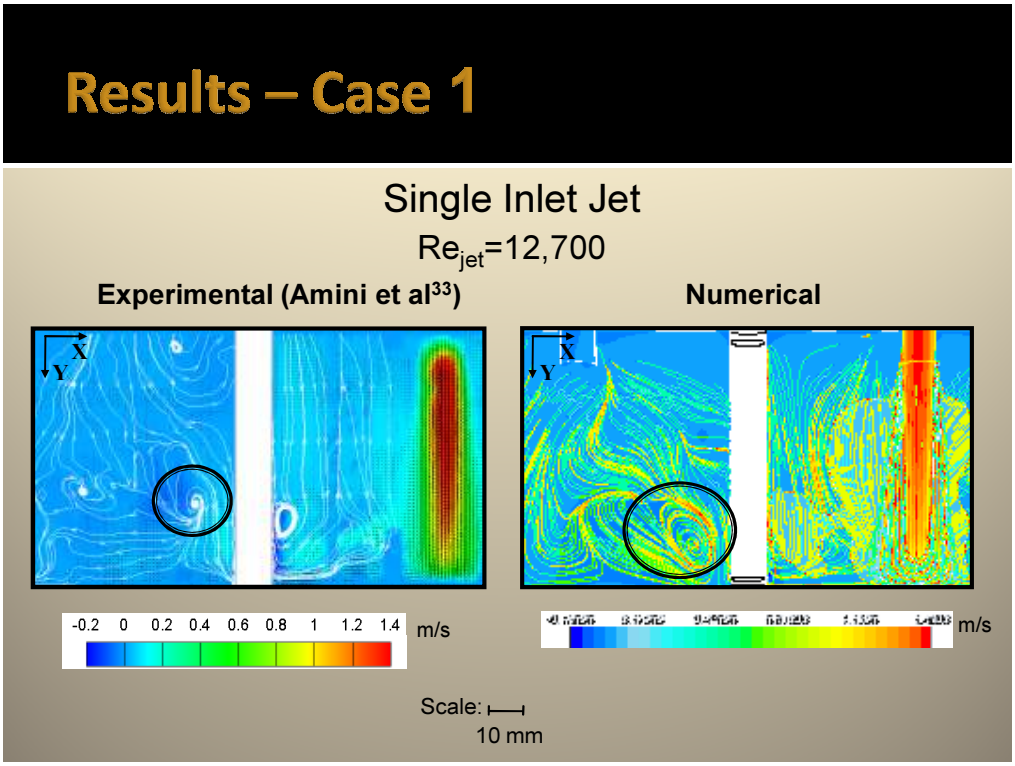

Figure 20 Numerical results along the experimental results for a single inlet jet of Re=12,700 along vertical mid-plane with Y-velocity component and streamlines present.

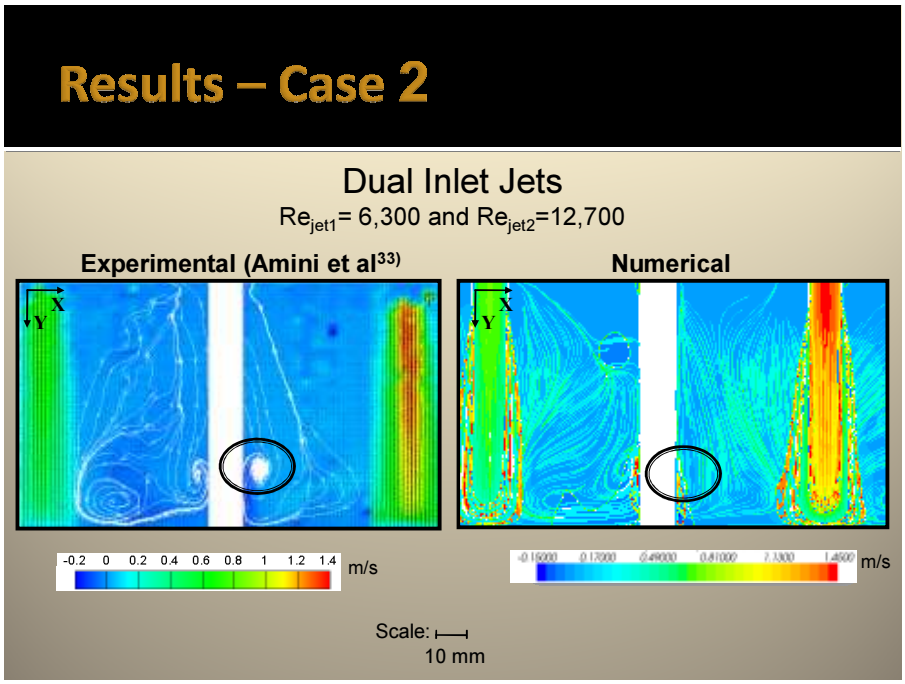

Figure 21 Numerical results along the experimental results for dual inlet jets of Re = 6,300 and Re=12,700 along vertical mid-plane with Y-velocity component and streamlines present.

5. MULTIPHASE FLOW COMPUTATIONAL FLUID DYNAMICS

The governing processes occurring in water reactors are without exception related to complex multiphase flows. Because of the large scales, inaccessibility and hostile high thermal conditions in and the reactor components, it is extremely difficult to obtain very detailed on line information of theses processes. Therefore, numerical simulation is a valuable tool in understanding, optimizing and designing the equipment. With the advance of affordable computing power and efficient parallel algorithms, multiphase flow computational fluid dynamics methods are now being applied to a wide class of industrial flow problems that were considered too complex only less than a decade ago. In water reactors, CFD models need to deal with multiphase flow of continuous phases and dispersed phases under boiling, condensation, deposition, entrainment and resuspension processes.

Multiphase flow computational techniques are complex. There are two basic types of models, i.e., *molecular models* on the subcontinuum scale (kinetic theory) and *continuum models* on micro/macroscale (continuum mechanics). For both approaches, the conservation laws are applied. However, historically the development of two-phase flow analysis has not followed any rigorous approach. Several computational algorithms are developed according to the situations and conditions. It is clear from Figure 19, the complexity of multiphase flow simulations. Clearly, in order to analyze multiphase (or just two-phase) flow systems, mathematical models, i.e., approximations to the actual flow phenomena have to be employed. Mixture models such as homogeneous (HEM) and drift flux models would simplify the mathematical formulation since the mixture properties can be used directly in the correlations for single-phase flow. Consequently, the HEM does not require the user to know the complex flow details. Less computer time is consumed than the separated flow models such as two-phase flow approach. , The most used approach in multiphase CFD is Eulerian-Eulerian two-fluid model.

Two-fluid model governing equations for k-phase (k = l (liquid) and g (gas)) are as follows:

Continuity:

$$\frac{\partial}{\partial t}\left(\alpha_k \rho_k\right) + \nabla \cdot \left(\alpha_k \rho_k \mathbf{u}_k\right) = \Gamma_k \tag{11}$$

Momentum conservation:

$$\frac{\partial}{\partial t}\left(\alpha_k \rho_k \mathbf{u}_k\right) + \nabla \cdot \left(\alpha_k \rho_k \mathbf{u}_k \mathbf{u}_k\right) = -\nabla\left(\alpha_k p_k\right) + \nabla \cdot \left[\alpha_k \left(\boldsymbol{\tau}_k + \boldsymbol{\tau}_k^T\right)\right] + \alpha_k \rho_k \mathbf{f}_k + \mathbf{M}_k \tag{12}$$

Energy conservation:

$$\begin{aligned} &\frac{\partial}{\partial t}\left[\alpha_k \rho_k \left(e_k + \tfrac{u_k^2}{2}\right)\right] + \nabla \cdot \left[\alpha_k \rho_k \left(e_k + \tfrac{u_k^2}{2}\right)\mathbf{u}_k\right] \\ &= -\nabla \cdot \left(\alpha_k p_k \mathbf{u}_k\right) + \nabla \cdot \left[\alpha_k \left(\boldsymbol{\tau}_k + \boldsymbol{\tau}_k^T\right) \cdot \mathbf{u}_k\right] - \nabla \cdot \left[\alpha_k \left(\mathbf{q}_k + \mathbf{q}_k^T\right)\right] + \alpha_k \rho_k \mathbf{f}_k \cdot \mathbf{u}_k + E_k \end{aligned} \tag{13}$$

where subscript k denotes either liquid (k=l) or gas (k=g) phase and α_k is local void fraction of k-phase. Also, Γ_k, $\mathbf{M}_k$, and E_k are mass, momentum, and energy transfer to the k-phase from the interface and $\boldsymbol{\tau}_k^T$ and $\mathbf{q}_k^T$ are k-phase turbulent momentum and heat flux. Note that ρ_k, $\mathbf{u}_k$, p_k, $\boldsymbol{\tau}_k$, $\mathbf{f}_k$, e_k and $\mathbf{q}_k$ are not instantaneous values. ρ_k, p_k, $\boldsymbol{\tau}_k$, and $\mathbf{q}_k$ denote k-phase-averaged density, pressure, shear stress, and heat flux, respectively and $\mathbf{u}_k$, $\mathbf{f}_k$, and e_k are mass-weighted velocity, body force per mass, and specific internal energy, respectively.

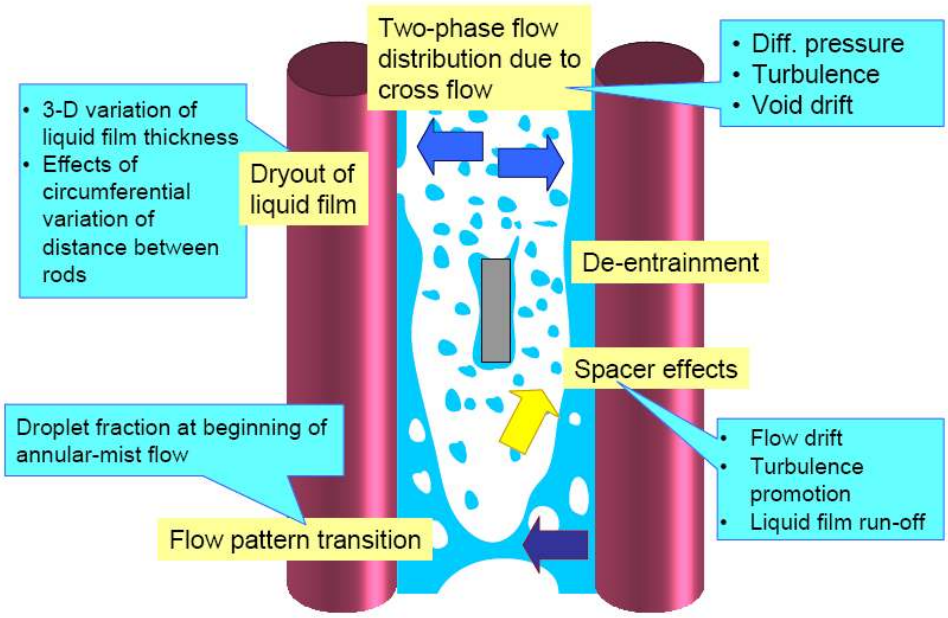

Figure 22 Complex multiphase flow patterns in reactor core

It should be indicated that the multiphase flow is primitive in that the correct formulation of the governing equations is still a subject of debate. For this reason too, the study of multiphase flows represents a challenging and potentially fruitful area of endeavor for scientist and engineers.

6. VERIFICATION AND VALIDATION

The first step in developing a standard for verifying and validating engineering computer models is to identify and define best practices. As a part of the contribution to common language, verification and validation are defined as:

- Verification is the process of determining that a computational model accurately represents the underlying mathematical model and its solution.
- Validation is the process of determining the degree to which a model is an accurate representation of the real world from the perspective of the intended use of the model.

Verification and validation together are the processes by which evidence is generated, and credibility is established that computer models have adequate accuracy and fidelity for their intended use.

It is clear that methods should be developed to verify engineering software and validate the results from models by comparing the results from simulations with experiments. Several guidelines were produced for the use of CFD in nuclear reactor safety applications. Details on verification and validation can be obtained by a book by P. Roach [28] and publications by W. Oberkampf et al [29,30].

7. CONCLUSIONS

Computational fluid dynamics (CFD) technique is a promising tool to reveal the physical mechanisms in fluid flow system. Recent enhancement of computer power and efficiency, and availability of CFD packages are fast extending into the nuclear industry. However, care should be taken due to the challenging problems of turbulence modeling and multiphase flow relations.

REFERENCES

1. INL (2003),'RELAP5-3D Code Manual', INEEL-EXT-98-00834.

2. Farvaque, M. (1992),'User's Manual of CATHARE 2 V1.3E'.

3. Odar, F. et al; (2005), 'TRACE V4.0 User's Manual' US NRC.

4. Bird, R.; Stewart, W. & Lightfoot, E. (2007), *Transport Phenomena*, John Wiley & Sons, Inc.

5. Pope, S. B. (2000), *Turbulent flows*, Cambridge University Press.

6. Chen, C & Jaw S., (1988), "Fundamentals of Turbulence Modeling" Taylor & Francis.

7. Barsamian, H. (2000),'New near-wall models with dynamic subgrid scale closure for large Eddy simulation in curviulinear coordinates for complex geometries', PhD thesis, Texas AM University.

8. Barsamian, H. & Hassan, Y. (2001), 'New wall modeling for complex flows using the large Eddy simulation technique in curvilinear coordinates', *International Journal of Heat and Mass Transfer* **44**(21), 4009-4026.

9. Hassan, Y. & Barsamian, H. (2004), 'Tube bundle flows with the large Eddy simulation technique in curvilinear coordinates', *International Journal of Heat and Mass Transfer* **47**, 3057-3071.

10. Leonard, A. (1974), 'Energy cascade in large-eddy simulations of turbulent fluid flows', *Advances in Geophysics* **18**(238), 237.

11. Smagorinsky, J (1963), 'General Circulation Experiments with the Primitive Equations', Monthly Weather Rev., 91,3, pp. 99-165.

12. Germano, M.; Piomelli U.; Moin, P. & Cabot, W. H. (1991) 'A Dynamic Subgrid-scale Eddy Viscosity Model' Physics of Fluids, A 3 (7), pp. 1760-1765.

13. Spalart, P.R.; Jou W. H.; Strelets M. And Allmaras S. R. (1997) 'Comments on the Feasibility of LES for Wings, and on a Hybrid RANS/LES Approach' 1st AFOSR Int. Conf. on DNS/LES, August 4-8, 1997, Ruston, LA. In: Advances in DNS/LES, C. Liu and Z. Liu Eds., Greyden Press, Columbia, Ohio, USA.

14. Spalart P. R. (2000) 'Strategies for Turbulence Modelling and Simulations' Int. J. of Heat and Fluid Flow, Vol. 21, pp. 252-263.

15. Wilcox, D.C. (1993), 'Turbulence Modeling for CFD', DCW Industries Inc., La Canada, CA.

16. ANSYS (2006),'ANSYS CFX-Solver Theory Guide', ANSYS, Inc., Canonsburg, PA, USA

17. Fluent (2003),'Fluent 6.1 Users Guide', Fluent Inc., Lebanon.

18. CD-adapco (1999),'Star-CD Manual', Computational Dynamics Ltd.

19. Cueto, O.; Emonot, P. & Ledac, P. (1996),'TRIO_U Manuel Utilisateur, Rep. DRN-DT', Commisariat a le energie atomique, Grenoble.

20. Bestion D, Guelfi A. Multiscale analysis of thermal hydraulics of nuclear reactors: the

NEPTUNE project. *SHF Meeting on Advances in the Modelling Methodologies of Two-phase Flows*, vol. 5, Lyon, France, 24–26 November 2005, La Houille Blanche.

21. Hohne, T.; Kliem, S. & Rohde U. (2005), ,CFD-Analysis of the Mixing Pattern under Various Flow Conditions at the ROCOM Test Facility using CFX-5' 13th International Conference on Nuclear Engineering, Beijing, China, May 16-20, 2005, ICONE 13-50524.

22. Hohne, T.; Kliema, S. & Biederb, U. (2006), 'Modeling of a buoyancy-driven flow experiment at the ROCOM test facility using the CFD codes CFX-5 and TrioU', *Nuclear Engineering and Design* **236**(12), 1309-1325.

23. Vijayaraghavan, V. K. (2006),'Turbulent Scalar Mixing in Single and Double Elbow Configurations', PhD thesis, Texas AM University

24. Vijayaraghavan, VK; Hassan, Y. & McFarland AR (2006), 'Turbulent Scalar Mixing in a Single and Double Elbow Configurations' Proceedings International Heat Transfer Conference, 13-18 August 2006, Sydney, Australia, Published by Begell Hose Inc. ISBN 1-56700-226-9.

25. Yuki K.; et al., (2004), "Prediction of the Wall Temperature Fluctuation in a T-Junction area with a 90-Degree Bend Upstream" the 6th International Conference on Nuclear Thermal Hydraulics, Operation and Safety (NUTHOS-6), Nara, Japan, October 4-8, 2004, paper ID, N6P082.

26. USNRC (1986), 'Feedwater Line Break, Information Notice 86-106', United States Nuclear Regulatory Commission.

27. USNRC (1987), 'Feedwater Line Break, Information Notice 86-106', United States Nuclear Regulatory Commission.

28. Roach, P. J. (1998), 'Verification and Validation in Computational Science and Engineering' Hermosa Publishers.

29. Oberkampf, W. L. & Trucano T. G. (2002), 'Verification and Validation in Computational Fluid Dynamics', Progress in Aerospace Sciences, Vol. 38, pp. 209-272.

30. Oberkampf, W. L.; Trucano T. G. & Hirsch C., (2004), 'Verification, Validation and Predictive Capability in Computational Engineering and Physics,' Applied Mechanics Reviews, Vol. 57, pp. 345-384.

31. Dominquez-Ontiveros, E.E., Estrada-Perez, C.E., Amini, N. and Hassan Y.A., "Jet Flow Mixing Measurements in the Vicinity of Rod Bundles Using PIV', presented at 2007 ANS/ENS International Meeting, November 11-15 2007, Washington DC, and Published in ANS Transaction, Vol.97, 2007.

32. Star-CCM+ Methodology and User Guide, Version 2.06.004, CD-Adapco Group

33. Amini N., Dominguez-Ontiveros E. E., Estrada Perez C. E., Fortenberry S. D. and Hassan Y. A., "PIV Measurements of Jet Flow Mixing in the Vicinity of Rod Bundles using Matched-Index of Refraction", ICONE16-48853, 2008
34. Nathaniel Salpeter and Hassan Y., "Numerical Simulation using Realizable K-E Turbulence Model of Jet Flow Mixing within Rod Bundles," ICONE-16-48854, May 11-15, 2008.